

Article

Activation of Peracetic Acid with Lanthanum Cobaltite Perovskite for Sulfamethoxazole Degradation under a Neutral pH: The Contribution of Organic Radicals

Xuefei Zhou, Haowei Wu, Longlong Zhang, Bowen Liang, Xiaoqi Sun and Jiabin Chen *

State Key Laboratory of Pollution Control and Resources Reuse, College of Environmental Science and Engineering, Tongji University, Shanghai 200092, China; zhouxuefei@tongji.edu.cn (X.Z.); wuhaowei@tongji.edu.cn (H.W.); 1810332@tongji.edu.cn (L.Z.); 1750564@tongji.edu.cn (B.L.); 1754021@tongji.edu.cn (X.S.)

* Correspondence: chenjiabin@tongji.edu.cn

Academic Editors: Marcello Brigante, Anan Yaghmur and Federico Totti
Received: 25 May 2020; Accepted: 11 June 2020; Published: 12 June 2020



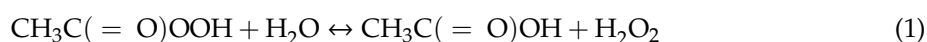
Abstract: Advanced oxidation processes (AOPs) are effective ways to degrade refractory organic contaminants, relying on the generation of inorganic radicals (e.g., $\bullet\text{OH}$ and $\text{SO}_4^{\bullet-}$). Herein, a novel AOP with organic radicals ($\text{R-O}\bullet$) was reported to degrade contaminants. Lanthanum cobaltite perovskite (LaCoO_3) was used to activate peracetic acid (PAA) for organic radical generation to degrade sulfamethoxazole (SMX). The results show that LaCoO_3 exhibited an excellent performance on PAA activation and SMX degradation at neutral pH, with low cobalt leaching. Meanwhile, LaCoO_3 also showed an excellent reusability during PAA activation. In-depth investigation confirmed $\text{CH}_3\text{C}(\text{O})\text{O}\bullet$ and $\text{CH}_3\text{C}(\text{O})\text{OO}\bullet$ as the key reactive species for SMX degradation in $\text{LaCoO}_3/\text{PAA}$ system. The presence of Cl^- (1–100 mM) slightly inhibited the degradation of SMX in the $\text{LaCoO}_3/\text{PAA}$ system, whereas the addition of HCO_3^- (0.1–1 mM) and humic acid (1–10 mg/L) could significantly inhibit SMX degradation. This work highlights the generation of organic radicals via the heterogeneous activation of PAA and thus provides a promising way to destruct contaminants in wastewater treatment.

Keywords: advanced oxidation processes (AOPs); peracetic acid; LaCoO_3 ; organic radicals

1. Introduction

Advanced oxidation processes (AOPs) have been extensively used to degrade toxic and bio-recalcitrant organic contaminants in wastewater treatment [1–8]. The commonly used AOPs are generally based on the in situ generation of highly reactive inorganic radicals, such as the hydroxyl radical ($\text{HO}\bullet$) and the sulfate radical ($\text{SO}_4^{\bullet-}$). They are usually generated through the homogeneous cleavage of the peroxide bond in inorganic peroxides, such as hydrogen peroxide (H_2O_2), peroxydisulfate (PDS) and peroxymonosulfate (PMS) [9]. The inorganic radicals possess high oxidation potential ($E^0 = 2.5\text{--}3.1$ V for $\text{SO}_4^{\bullet-}$ and $E^0 = 1.9\text{--}2.7$ V for $\text{HO}\bullet$) [10] and thus can effectively destruct a wide range of organic contaminants with the second-order rate constants ranging from 10^5 to 10^9 $\text{M}^{-1} \text{s}^{-1}$ for $\text{SO}_4^{\bullet-}$ [11] and from 10^7 to 10^{10} $\text{M}^{-1} \text{s}^{-1}$ for $\text{HO}\bullet$ [12]. However, the short half-life (30–40 μs for $\text{SO}_4^{\bullet-}$, 1 μs for $\text{HO}\bullet$) of inorganic radicals may reduce the possibility of their interaction with the target contaminants [13,14]. On the other hand, the non-selectivity of inorganic radicals render them susceptible to consumption by the water matrices, e.g., anions and natural organic matters. These drawbacks reduce the degradation efficiency of target contaminants by inorganic radicals in real wastewater treatment [15].

Recently, an emerging AOP mainly based on the organic radicals ($R-O^\bullet$) has become an attractive alternative for organic contaminant degradation in wastewater treatment. Organic radicals are commonly generated from the activation of peroxide bond in the organic peroxy acid, such as peracetic acid (PAA, $CH_3C(O)OOH$) [16,17]. PAA is known as a broad-spectrum antimicrobial agent and has been widely used as an alternative to conventional chlorine disinfectants in wastewater disinfection, owing to the advantages of PAA, such as strong oxidation power (redox potential ranging from 1.06 to 1.96 V) [18] and a low potential of harmful disinfection byproduct generation [19–21]. PAA is produced by the reaction of acetic acid and H_2O_2 in the presence of a strong acid catalyst, such as sulfuric acid [22–24], and thus the commercial PAA solution is an equilibrium solution with acetic acid and H_2O_2 according to Equation (1).



PAA can directly oxidize some organic contaminants in wastewater treatment, e.g., amino acid [25] and β -lactam antibiotics [26]. After the introduction of intensive energy (e.g., heat and UV) or catalysts, the peroxide bond in PAA can be activated to produce reactive species (e.g., HO^\bullet and $R-O^\bullet$) [19,27–29]. Compared with the inorganic peroxides, e.g., H_2O_2 (213 kJ mol^{-1}), PAA has a weaker $-O-O-$ bond (159 kJ mol^{-1} for PAA [26,30]), which can be easily activated for intensive radical generation to attack target contaminants, such as pharmaceuticals [19,31], phenols [27,32], and dyes [33]. Therefore, PAA shows a great potential to be an ideal alternative to H_2O_2 in AOPs and the development of efficient and environmentally friendly methods to activate PAA is of great significance.

Many attempts have been made to develop effective strategies for the activation of PAA. Among them, transition metal ions have been reported as the most viable activators. For example, iron and cobalt ions showed a great performance for the activation of PAA to degrade organic contaminants [31,34]. However, one of the serious hindrances to this homogeneous processes was the poor reusability and potential toxicity of some metal ions [35]. A heterogeneous catalyst containing cobalt with low cobalt leaching and high reusability is expected to overcome these problems. In this work, a Co-based perovskite ($LaCoO_3$) was used to activate PAA to eliminate recalcitrant contaminants. Perovskite, with the ABO_3 structure, has recently attracted considerable interests in the field of material science and heterogeneous catalysis [36,37], due to the flexible chemical composition, element abundance and structural stability. In particular, perovskite oxides are regarded as excellent catalysts in wastewater treatment. For example, $LaCoO_3$ has been used as a catalyst to activate PMS or H_2O_2 for contaminant degradation [36,38–40]. However, the performance of $LaCoO_3$ on PAA activation and the mechanisms underlying the $LaCoO_3^-$ activated PAA reaction are still unknown.

Herein, $LaCoO_3$ perovskite was synthesized via the sol-gel method and then used to activate PAA to degrade sulfamethoxazole (SMX). The aims of this study were: 1) to investigate the performance of $LaCoO_3$ /PAA on the degradation of SMX; 2) to evaluate the impact of water matrices on SMX degradation in the activated PAA process; 3) to identify the reactive radical species dominated in the contaminant degradation; 4) to reveal the activation mechanism of PAA by $LaCoO_3$. To our best knowledge, this study is among the first to investigate the activation of PAA by perovskite and elucidate the mechanism for organic radical generation.

2. Results

2.1. Characterization of $LaCoO_3$

Figure 1a shows the X-ray powder diffraction (XRD) pattern of $LaCoO_3$. The diffraction peaks at 2θ values of 23.30° , 32.83° , 33.29° , 39.76° , 40.13° , 47.68° , 52.71° , 53.66° , 59.08° , 59.93° and 68.95° correspond to miller indices values of (012), (110), (104), (202), (006), (024), (122), (116), (214), (018) and (220), respectively [38]. In addition, the morphological properties of $LaCoO_3$ was analyzed by Transmission Electron Microscope (TEM). The TEM image (Figure 1b) shows a disordered microstructure of the porous $LaCoO_3$ nanospheres, with the average particle size approximately 23 nm according to the

transmission electron microscope (TEM) image. The selected-area electron diffraction (SAED) pattern in Figure 1c revealed that the LaCoO_3 nanospheres were polycrystalline. The Brunauer–Emmett–Teller (BET) area of the sample was obtained to be $14 \text{ m}^2/\text{g}$ and the zeta potential of LaCoO_3 was determined to be 6.1.

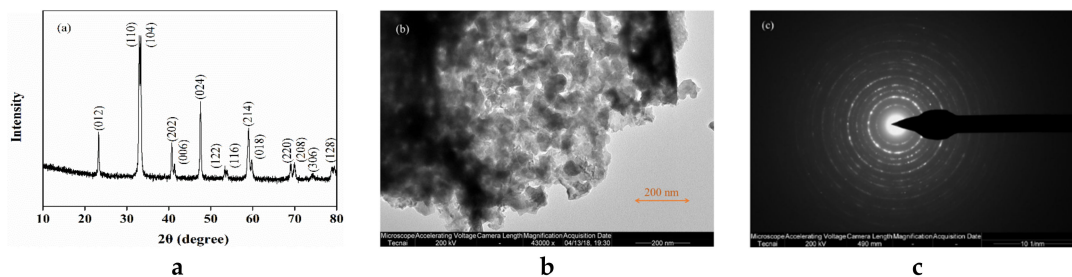


Figure 1. (a) X-ray powder diffraction (XRD) pattern, (b) transmission electron microscope (TEM) image and (c) selected-area electron diffraction (SAED) image of the LaCoO_3 .

2.2. Degradation of SMX by PAA Activated with LaCoO_3

The prepared LaCoO_3 was used to activate PAA for the degradation of SMX. As shown in Figure 2, the loss of SMX was not observed in the presence of LaCoO_3 alone, indicating the negligible adsorption of SMX on LaCoO_3 . SMX was slightly degraded after the addition of PAA alone, suggesting the slight reactivity of PAA towards SMX. However, SMX could be almost completely degraded within 60 min in the presence of PAA and LaCoO_3 ; hence, LaCoO_3 and PAA showed a synergistic effect on SMX degradation. It should be addressed that the removal efficiency of SMX achieved by $\text{LaCoO}_3/\text{PAA}$ in this study was comparable or even higher than many published studies [41–46], and with much less catalyst addition. For example, Yan et al. [46] prepared $\text{CuO@Al}_2\text{O}_3$ to activate PMS and approximately 90% of SMX was removed under similar conditions ($[\text{SMX}]_0 = 39.5 \mu\text{M}$, $[\text{PMS}]_0 = 0.4 \text{ mM}$, pH 6.2) but a large catalyst dosage ($[\text{cata}]_0 = 500 \text{ mg/L}$). Lalas et al. [45] reported that complete SMX degradation was obtained within 90 min through persulfate with 2 g immobilized CuOx catalyst. The LaCoO_3 was reported as an excellent catalyst for the activation of peroxides, such as H_2O_2 and PMS, to generate reactive species to degrade contaminants [39,47,48]. It was most likely to activate PAA to degrade SMX. It is noted that commercial PAA solution always contains a certain amount of H_2O_2 during preparation; we thus evaluated the contribution of H_2O_2 to SMX degradation in the $\text{LaCoO}_3/\text{PAA}$ system. As Figure 2 shows, the degradation of SMX was negligible in the presence of H_2O_2 , or $\text{H}_2\text{O}_2/\text{LaCoO}_3$, where H_2O_2 concentration was equivalent to that in PAA solution. Hence, the degradation of SMX in $\text{LaCoO}_3/\text{PAA}$ was not affected by H_2O_2 in PAA solution. Meanwhile, this result also indicated that PAA was more easily activated by LaCoO_3 than H_2O_2 . Indeed, the peroxide bond energy in PAA was reported to be 159 kJ mol^{-1} , which is lower than that in H_2O_2 (213 kJ mol^{-1}) [31]. Hence, the dissociation of peroxide bond in PAA to generate reactive species is thermally feasible and even likely more easily than H_2O_2 .

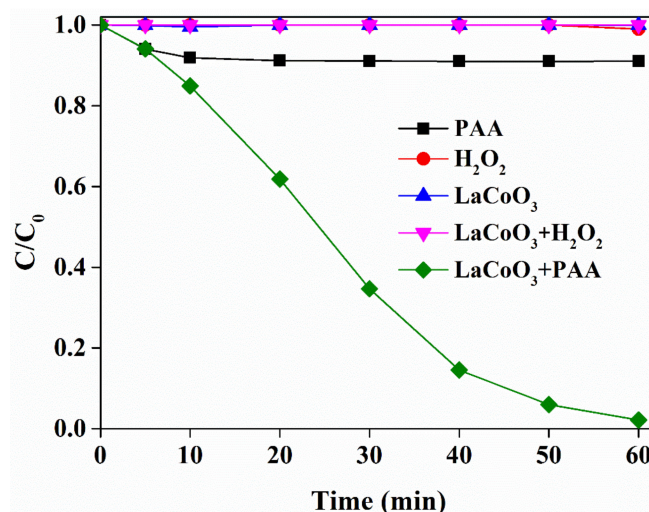


Figure 2. Sulfamethoxazole (SMX) degradation in different systems. LaCoO₃ = 20 mg/L, SMX = 50 μM, peracetic acid (PAA) (or H₂O₂) = 660 μM, pH 7, 25 °C.

2.3. Effects of Catalyst Loadings

The effect of catalyst loading on the SMX degradation in the LaCoO₃/PAA system was evaluated and the results are shown in Figure 3. Noting that the adsorption of SMX on LaCoO₃ was negligible even in the presence of 0.1g/L LaCoO₃ (data not shown), the removal of SMX could be attributed to the oxidative degradation rather than adsorption in the LaCoO₃/PAA system. The degradation of SMX was gradually increased with the increasing loadings of LaCoO₃ from 10 to 50 mg/L. A higher loading of LaCoO₃ could supply more active sites for PAA to generate reactive species for contaminant degradation. When the LaCoO₃ loading further increased to 100 mg/L, the degradation of SMX was only slightly increased. Hence, high loading of LaCoO₃ had excess reactive sites for PAA activation, and even likely to quench the reactive species generated from PAA activation. Therefore, the excess loading of LaCoO₃ could not further enhance the PAA activation.

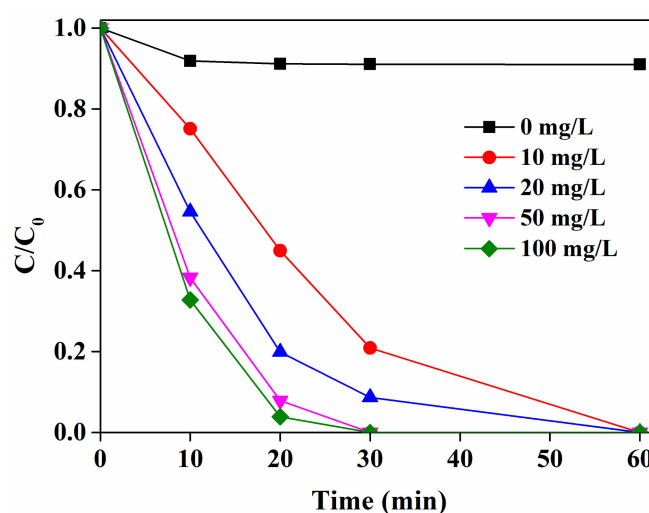


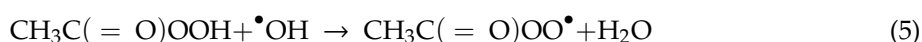
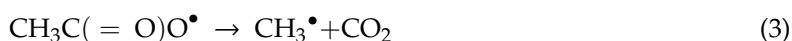
Figure 3. Effect of LaCoO₃ loading on SMX degradation in the LaCoO₃/PAA system. SMX = 50 μM, PAA = 660 μM, pH 7, 25 °C.

2.4. Activation Mechanism

To get insight into the degradation of SMX in the LaCoO₃/PAA system, the reactive species generated from PAA activation by LaCoO₃ was comprehensively studied. Ascorbic acid (AA) is a common scavenger for reactive radicals, and thus is widely used for investigating radical contributions

in contaminant degradation [33]. As can be seen in Figure 4a, the presence of AA significantly inhibited the degradation of SMX in the LaCoO₃/PAA system, and the degradation rates decreased from 98.9% to 3.8% with the concentration of AA increased from 0 to 0.5 mM. This result indicated that the radical species contributed to the degradation of SMX in the LaCoO₃/PAA system.

Generally, the activation of PAA could generate various reactive radical species, mainly including •OH, CH₃C(=O)O•, CH₃C(=O)OO•, CH₃• and CH₃O₂• (Equations (2–6)) [30].



Some radical species might contribute to the contaminant degradation in the activated PAA system. For example, •OH contributed to the degradation of carbamazepine and ibuprofen in the UV/PAA system, whereas a strong reactivity of CH₃C(=O)O• and/or CH₃C(=O)OO• was observed in the oxidation of certain naphthyl compounds, such as naproxen and 2-naphthoxyacetic acid [19].

The quenching experiments were further conducted to reveal which radicals were the main reactive species contributed to SMX degradation in the LaCoO₃/PAA system. *Tert*-butanol (TBA) is a desired quenching agent to distinguish the contribution of •OH in the activation of PAA because TBA is highly reactive towards •OH ($k = 6.0 \times 10^8 \text{ M}^{-1} \text{ s}^{-1}$), but was inert towards other R-O•. Noting that the rate constants between SMX and •OH is $7.9 \times 10^9 \text{ M}^{-1} \text{ s}^{-1}$, the contribution of •OH can be almost completely consumed when the concentration of TBA is 1000 times higher than that of SMX. As shown in Figure 4a, the presence of excess TBA (500 mM) slightly inhibited the degradation of SMX in PAA/LaCoO₃ system, indicating that •OH played a negligible role in LaCoO₃/PAA system for SMX degradation. Moreover, MeOH is regarded as a common scavenger for •OH ($k = 6.0 \times 10^8 \text{ M}^{-1} \text{ s}^{-1}$), and has been recently reported as a scavenger for organic radicals (R-O•) in the activated PAA [31]. Therefore, the addition of excess MeOH could be used to evaluate the contributions of R-O• under the premise of TBA quenching results. In contrast to TBA, the addition of MeOH could significantly suppress the degradation of SMX in the LaCoO₃/PAA system, indicating that the formed R-O• might play a major role in SMX degradation.

To further validate the contributions of CH₃• and CH₃O₂•, N₂ was pumped into the reaction solution. Because CH₃• can quickly react with oxygen to form CH₃O₂• (Equation (4), $k = (2.8\text{--}4.1) \times 10^9 \text{ M}^{-1} \text{ s}^{-1}$), the contribution of CH₃• and CH₃O₂• could be determined when the dissolved oxygen (DO) was excluded in the presence of high purity N₂. The concentration of DO was determined to decrease from 4.95 mg/L to 0.21 mg/L after N₂ purging. As shown in Figure 4b, the purging of N₂ showed a negligible inhibition effect on SMX degradation, suggesting that the contributions of CH₃• and CH₃O₂• to SMX degradation could be ignored. Therefore, CH₃C(=O)O• and CH₃C(=O)OO• were speculated to be the primary organic radical species that contributed to SMX degradation in the LaCoO₃/PAA system.

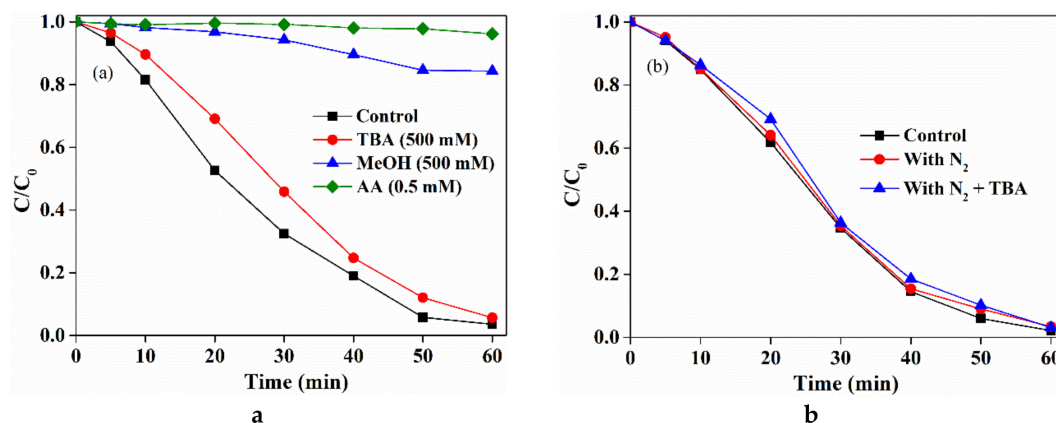


Figure 4. (a) Effect of ascorbic acid (AA), *tert*-butanol (TBA) and MeOH, and (b) Dissolved oxygen (DO) on the degradation of SMX in the $LaCoO_3/PAA$ system. $LaCoO_3 = 20$ mg/L, SMX = 50 μ M, PAA = 660 μ M, pH 7, 25 $^{\circ}$ C.

The leaching of Co from $LaCoO_3$ during the reaction was detected. After 60 min, the leached Co in the solution was determined to be 0.13 mg/L, which is much lower than the required concentration (<1 mg/L) in the Environmental Quality Standards for Surface Water in China. In order to further investigate whether the leached Co contributed to the PAA activation for SMX degradation, PAA was introduced to the leached solution, and the result show that the degradation of SMX was not observed. Hence, the degradation of SMX in $LaCoO_3/PAA$ originated from the heterogeneous activation of PAA by $LaCoO_3$ rather than the homogeneous activation with the leached Co ions. The heterogeneous activation of PAA with $LaCoO_3$ was proposed in Figure 5. PAA was first adsorbed on the surface of $LaCoO_3$, and then activated by the Co on the B site of perovskite to generate organic radicals, e.g., CH_3COO^{\bullet} , which could act as an oxidant for SMX degradation. Meanwhile, Co(II) was oxidized to Co(III) after PAA activation (Equation (7)) [31,49,50]. The decomposition of CH_3COO^{\bullet} can generate CO_2 and CH_3^{\bullet} , which could further react with oxygen to generate CH_3OO^{\bullet} . The generated CH_3^{\bullet} and CH_3OO^{\bullet} showed low reactivity towards contaminants. On the other hand, Co(III) further reacted with PAA to generate CH_3COOO^{\bullet} (Equation (8)), another effective reactive organic radical contributed to the rapid oxidation of SMX; while Co(III) was reduced to Co(II), and further participated in the PAA activation. Overall, Co acted as a catalyst role in the PAA activation to generate $CH_3C(=O)O^{\bullet}$ and $CH_3C(=O)OO^{\bullet}$ for SMX oxidation.

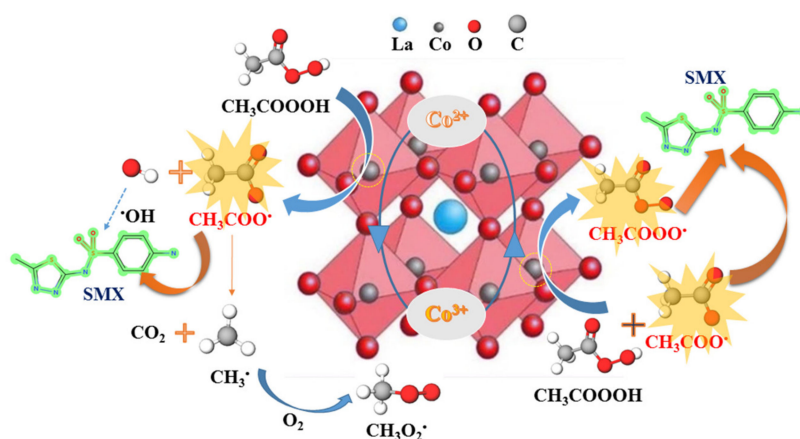


Figure 5. Proposed mechanism of PAA activated by $LaCoO_3$.

2.5. Effects of Water Matrices

The effects of water matrices, such as common anions and natural organic matter, were evaluated on SMX degradation in the LaCoO₃/PAA system. As shown in Figure 6a, the presence of Cl⁻ (0–20 mM), a pervasive anion in natural water, slightly inhibited the degradation of SMX in the LaCoO₃/PAA system. Cl⁻ is a common radical scavenger in AOPs and can react with the radical species to generate less reactive chlorine radicals, such as Cl[•] and Cl₂^{•-}. The consumption of reactive radicals by Cl⁻ could reduce the reaction between R-O[•] with SMX and thus reduce the degradation efficiency of SMX.

HCO₃⁻/CO₃²⁻ was reported as a common radical scavenger in PMS-based AOPs and the Co(II)/PAA system [51]; thus, the effects of HCO₃⁻/CO₃²⁻ on the degradation of SMX was also studied in the LaCoO₃/PAA system. As shown in Figure 6b, HCO₃⁻/CO₃²⁻ could significantly inhibit the SMX oxidation in the LaCoO₃/PAA system, and the inhibitory effect rapidly increased with an increasing concentration of HCO₃⁻/CO₃²⁻. Noting that the reaction was maintained at pH 7.0 with phosphate buffer, HCO₃⁻ is the dominant species in the system due to the pK_{a1} = 6.4. Although HCO₃⁻ can significantly quench [•]OH, [•]OH just played a minor role in the LaCoO₃/PAA system for SMX degradation. Meanwhile, HCO₃⁻ was reported to show very low reactivity towards R-O[•], according to the phenomenon that the contaminant degradation in the UV/PAA + TBA system was not affected by HCO₃⁻ [19]. Thus, the reactions between HCO₃⁻ and the reactive radicals ([•]OH and R-O[•]) would not be the primary reason for the significant inhibition of SMX degradation in the LaCoO₃/PAA system. The inhibitory effect could be attributed to the influence of HCO₃⁻ on the interaction between PAA and LaCoO₃ by competitive adsorption.

The effects of natural organic matter on SMX degradation were studied by adding a certain amount of humic acid (HA) in the LaCoO₃/PAA system. As shown in Figure 6c, the presence of HA (0–10 mg/L) showed an apparent inhibition on SMX degradation in the LaCoO₃/PAA system. To be specific, the degradation of SMX significantly decreased from 100% to 51% after 50 min as the concentration of HA increased from 0 to 10 mg/L. HA was previously reported to react with R-O[•], with the rate constants reaching 10⁴ L mg⁻¹ s⁻¹. Hence, the addition of HA could compete with SMX towards R-O[•] and thus reduce the degradation efficiency of SMX in the LaCoO₃/PAA system.

The impact of real water matrices on the degradation of SMX was further explored in LaCoO₃/PAA. The characteristics of the surface water (SW) and wastewater (WW) were listed in Table 1. As shown in Figure 6d, the degradation of SMX was inhibited in SW and WW, with the degradation efficiency moderately decreased to 90% and 85% after 60 min, respectively. Hence, some matrices in the real water sample might impose an adverse effect on SMX degradation in the LaCoO₃/PAA system. Based on the above analysis, the slight inhibition that occurred in SW and WW matrices was likely to primarily contribute to the scavenging of R-O[•] by organic matters.

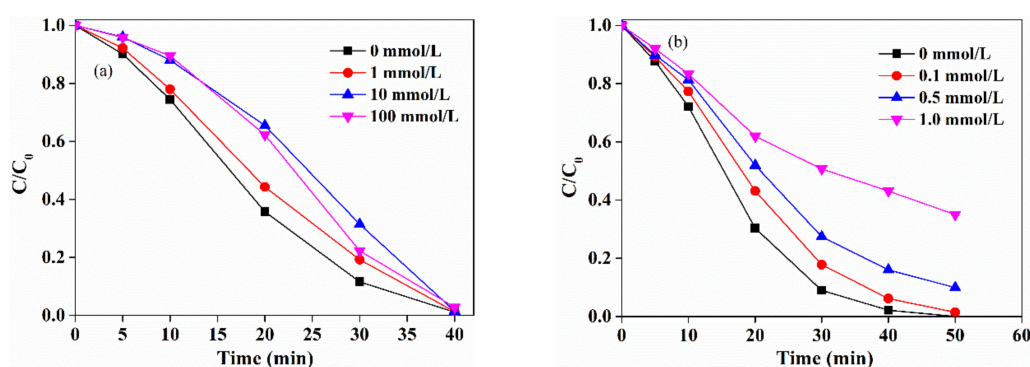


Figure 6. Cont.

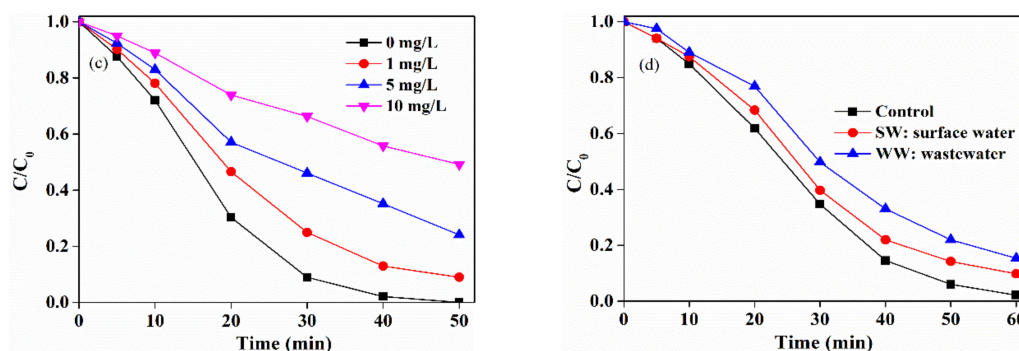


Figure 6. Effect of (a) Cl^- , (b) HCO_3^- , (c) humic acid and (d) real water on the degradation of SMX by the $\text{LaCoO}_3/\text{PAA}$ system. $\text{LaCoO}_3 = 20 \text{ mg/L}$, $\text{SMX} = 50 \text{ }\mu\text{M}$, $\text{PAA} = 660 \text{ }\mu\text{M}$, $\text{pH} 7.0$, $25 \text{ }^\circ\text{C}$.

Table 1. Characteristics of water samples.

Sample	TN (mg/L)	TP (mg/L)	pH	UV254	TOC (mg/L)	Cl^- (mg/L)
SW	0.81	0.07	7.8	0.13	3.1	32.6
WW	11.1	0.84	7.1	0.41	10.6	92.3

Note: SW: surface water; WW: wastewater.

2.6. Reusability of LaCoO_3

The reusability is crucial for the application of a catalyst in the heterogeneous reactions. LaCoO_3 was reused to evaluate its performance on PAA activation after the reaction. As shown in Figure 7, an excellent performance of LaCoO_3 in PAA activation to degrade SMX was still observed after four runs. Almost all SMX was completely removed in each run with a slight downward trend in the removal rates (from 98% in the 1st run to 95% in the 4th run). Moreover, the low leaching of Co under a neutral pH condition after the reaction by about 60 min also indicated the high structural stability of the prepared LaCoO_3 during the reaction. Hence, the prepared LaCoO_3 showed a high structural and chemical stability in PAA activation for the degradation of SMX.

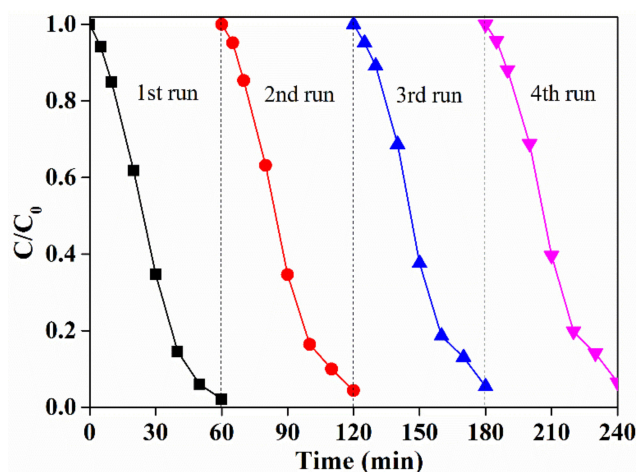


Figure 7. Reusability of LaCoO_3 . $\text{LaCoO}_3 = 20 \text{ mg/L}$, $\text{SMX} = 50 \text{ }\mu\text{M}$, $\text{PAA} = 660 \text{ }\mu\text{M}$, $\text{pH} 7.0$, $25 \text{ }^\circ\text{C}$. black square: 1st run, red circle: 2nd run, blue up triangle: 3rd run, magenta down triangle: 4th run.

3. Materials and Methods

3.1. Chemicals and Reagents

PAA solution (39% PAA and 6% H_2O_2 w/w), hydrogen peroxide solution (30% H_2O_2 w/w), sulfamethoxazole (SMX), cobaltous sulfate (CoSO_4), cobaltous acetylacetonate ($\text{Co}(\text{C}_5\text{H}_7\text{O}_2)_2$), and

cobalt acetylacetonate ($\text{Co}(\text{C}_5\text{H}_7\text{O}_2)_3$) were purchased from Sigma-Aldrich (St. Louis, MO, USA). Oxone ($\text{KHSO}_5 \cdot 0.5\text{KHSO}_4 \cdot 0.5\text{K}_2\text{SO}_4$) and lanthanum nitrate hexahydrate ($\text{La}(\text{NO}_3)_3 \cdot 6\text{H}_2\text{O}$) were purchased from Aladdin Industrial Corporation. Cobalt nitrate hexahydrate ($\text{Co}(\text{NO}_3)_2 \cdot 6\text{H}_2\text{O}$), citric acid monohydrate ($\text{C}_6\text{H}_8\text{O}_7 \cdot \text{H}_2\text{O}$), sodium sulfate (Na_2SO_4), sodium nitrate (NaNO_3), sodium chloride (NaCl), sodium bicarbonate (NaHCO_3), ascorbic acid (AA), methanol (MeOH), and *tert*-butanol (TBA) were purchased from Sinopharm Chemical Reagent Co., Ltd., China. All solutions were prepared with ultrapure water from a Milli-Q academic (Millipore) system (MILLI-Q® INTEGRAL 5, 18.2 M Ω cm).

3.2. Preparation and Characterization of LaCoO_3

LaCoO_3 was synthesized by a sol-gel process. Briefly, the mixtures of metal nitrates and citric acid were stirred for 12 h and then heated at 100 °C to remove water in the oil bath. The resultant sticky gel was subsequently oven-dried at 100 °C overnight. The obtained spongy material was then grinded into fine powders and calcined for 7 h in a muffle furnace to form the desired perovskite structure. After cooling, the sample was washed and dried overnight.

Transmission electron microscope (TEM) and selected-area electron diffraction (SAED) patterns were conducted on the field emission transmission electron microscope (Tecnai G2 F30, Eindhoven, Holland). The X-ray powder diffraction (XRD) analysis was characterized by Cu K α irradiation ($\lambda = 1.5406 \text{ \AA}$) (Bruker D8-Advance, Karlsruhe, Germany). The surface area of LaCoO_3 was analyzed by a Brunauer–Emmett–Teller (BET) analyzer (Micrometrics ASAP 2020, Norcross, GA, USA). The zeta potential analysis was acquired through a Malvern Zetasizer with a Zetasizer (Nano ZS90, Malvern, UK) at 25 °C.

3.3. Experimental Procedures

The batch experiments were conducted in 100 mL amber glass bottles. The solution was mixed by magnetic stirring at room temperature (25 °C). The reactions were initiated by adding PAA (660 μM) to the solution containing SMX (50 μM) and LaCoO_3 (20 mg/L). Sample aliquots were taken at the predetermined time intervals and subsequently quenched with excess $\text{Na}_2\text{S}_2\text{O}_3$ immediately. Afterwards, the quenched sample was filtered through a 0.22 μm membrane and analyzed within 24 h. The initial pH of the solution was adjusted by H_2SO_4 and NaOH to the designated value. Control experiments without PAA or LaCoO_3 were conducted to evaluate the contributions of PAA or LaCoO_3 alone for the degradation of SMX. Radical scavenging experiments were conducted with addition of 500 mM of alcohols (*tert*-butyl alcohol (TBA) or methanol (MeOH)). In order to assess the reusability of LaCoO_3 in the activation of PAA, the catalyst was collected by centrifugation and then washed with methanol and ultrapure water. Afterwards, the solid was dried at 60 °C overnight and four runs were carried out to evaluate the reusability. All the experiments were conducted in duplicate or more.

3.4. Analytical Methods

SMX was analyzed by high-performance liquid chromatography (HPLC 1290, Agilent Technology, Santa Clara, CA, USA) equipped with a Zorbax SB-C18 column (4.6 \times 250 mm, 5 μm) and a UV detector at a wavelength of 265 nm. The flow rate was set at 1 mL min^{-1} and the injection was set at 20 μL . The mobile phase was the mixture of acetonitrile and water containing 0.4% acetic acid (70:30).

The PAA concentration in the solution was quantified by the *N,N*-diethyl-*p*-phenylenediamine (DPD) colorimetric method [19]. Briefly, the PAA solution was sampled and then was immediately mixed with excess KI (60 mM), DPD (2.8 mM), and phosphate buffer (0.5 M at pH 6.5) and measured at 515 nm on a UV-visible spectrophotometer (Beckman DU 520, Beckman Coulter, Inc., Fullerton, CA, USA).

4. Conclusions

LaCoO_3 was successfully synthesized and used for PAA activation to degrade SMX. The rapid degradation of SMX was observed with the heterogeneous activation of PAA by LaCoO_3 under a

neutral pH condition. Cl^- was slightly inhibited by the degradation of SMX, whereas HCO_3^- and HA significantly reduce SMX in the $\text{LaCoO}_3/\text{PAA}$ system. LaCoO_3 showed high structural stability and reusability after consecutive runs with low Co leaching under a neutral condition. Organic radicals, e.g., $\text{CH}_3\text{C}(=\text{O})\text{O}^\bullet$ and $\text{CH}_3\text{C}(=\text{O})\text{OO}^\bullet$ were proposed as the primary radical species responsible for SMX degradation in the $\text{LaCoO}_3/\text{PAA}$ system. This work provides an emerging AOP relying on organic radicals to degrade organic contaminants in the wastewater treatment.

Author Contributions: X.Z. and J.C. conceived and designed the experiments; H.W., B.L., and X.S. performed the experiments; H.W. and L.Z. analyzed the data; X.Z. and J.C. contributed reagents/materials/analysis tools; J.C. and L.Z. wrote the paper. All authors have read and agreed to the published version of the manuscript.

Funding: This research was funded by Shanghai Science and Technology Committee (19DZ1208400), and the National Natural Science Foundation of China (51878431).

Conflicts of Interest: The authors declare no conflicts of interest.

References

1. Oturan, M.A.; Aaron, J.-J. Advanced Oxidation Processes in Water Wastewater Treatment Principles and Applications A Review. *Crit. Rev. Environ. Sci. Tech.* **2014**, *44*, 2577–2641. [[CrossRef](#)]
2. Zhou, D.; Chen, L.; Li, J.; Wu, F. Transition metal catalyzed sulfite auto-oxidation systems for oxidative decontamination in waters: A state-of-the-art minireview. *Chem. Eng. J.* **2018**, *346*, 726–738. [[CrossRef](#)]
3. Xie, P.; Ma, J.; Liu, W.; Zou, J.; Yue, S.; Li, X.; Wiesner, M.R.; Fang, J. Removal of 2-MIB and geosmin using UV/persulfate: Contributions of hydroxyl and sulfate radicals. *Water Res.* **2015**, *69*, 223–233. [[CrossRef](#)] [[PubMed](#)]
4. Lei, X.; You, M.; Pan, F.; Liu, M.; Yang, P.; Xia, D.; Li, Q.; Wang, Y.; Fu, J. $\text{CuFe}_2\text{O}_4/\text{GO}$ nanocomposite as an effective and recoverable catalyst of peroxymonosulfate activation for degradation of aqueous dye pollutants. *Chin. Chem. Lett.* **2019**, *30*, 2216–2220. [[CrossRef](#)]
5. Ma, M.; Chen, L.; Zhao, J.; Liu, W.; Ji, H. Efficient activation of peroxymonosulfate by hollow cobalt hydroxide for degradation of ibuprofen and theoretical study. *Chin. Chem. Lett.* **2019**, *30*, 2191–2195. [[CrossRef](#)]
6. Liu, T.; Yin, K.; Liu, C.; Luo, J.; Crittenden, J.; Zhang, W.; Luo, S.; He, Q.; Deng, Y.; Liu, H. The role of reactive oxygen species and carbonate radical in oxcarbazepine degradation via UV, UV/ H_2O_2 : Kinetics, mechanisms and toxicity evaluation. *Water Res.* **2018**, *147*, 204–213. [[CrossRef](#)]
7. Glaze, W.H.; Kang, J.W.; Chapin, D.H. The Chemistry of Water Treatment Processes Involving Ozone, Hydrogen Peroxide and Ultraviolet Radiation. *Ozone Sci. Eng.* **1987**, *9*, 335–352. [[CrossRef](#)]
8. Glaze, W.H.; Kang, J.W. Advanced oxidation processes. Description of a kinetic model for the oxidation of hazardous materials in aqueous media with ozone and hydrogen peroxide in a semibatch reactor. *Ind. Eng. Chem. Res.* **1989**, *28*, 1573–1580. [[CrossRef](#)]
9. Duan, P.; Qi, Y.; Feng, S.; Peng, X.; Wang, W.; Yue, Y.; Shang, Y.; Li, Y.; Gao, B.; Xu, X. Enhanced degradation of clothianidin in peroxymonosulfate/catalyst system via core-shell $\text{FeMn}@\text{N-C}$ and phosphate surrounding. *Appl. Catal. B Environ.* **2020**, *267*, 118717. [[CrossRef](#)]
10. Rehman, F.; Sayed, M.; Khan, J.A.; Shah, N.S.; Khan, H.M.; Dionysiou, D.D. Oxidative removal of brilliant green by UV/ $\text{S}_2\text{O}_8^{2-}$, UV/ HSO_5^- and UV/ H_2O_2 processes in aqueous media: A comparative study. *J. Hazard. Mater.* **2018**, *357*, 506–514. [[CrossRef](#)]
11. Oh, W.-D.; Dong, Z.; Lim, T.-T. Generation of sulfate radical through heterogeneous catalysis for organic contaminants removal: Current development, challenges and prospects. *Appl. Catal. B Environ.* **2016**, *194*, 169–201. [[CrossRef](#)]
12. Haag, W.R.; Yao, C.C.D. Rate constants for reaction of hydroxyl radicals with several drinking water contaminants. *Environ. Sci. Tech.* **1992**, *26*, 1005–1013. [[CrossRef](#)]
13. Chen, J.B.; Fang, C.; Xia, W.J.; Huang, T.Y.; Huang, C.H. Selective Transformation of β -Lactam Antibiotics by Peroxymonosulfate: Reaction Kinetics and Non-Radical Mechanism. *Environ. Sci.* **2018**, *52*, 1461–1470. [[CrossRef](#)] [[PubMed](#)]
14. Cao, J.Y.; Song, L. Degradation of tetracycline by peroxymonosulfate activated with zero-valent iron: Performance, intermediates, toxicity and mechanism. *Chem. Eng. J.* **2019**, *364*, 45–56. [[CrossRef](#)]

15. Tsitonaki, A.; Petri, B.; Crimi, M.; Mosbk, H.; Siegrist, R.L.; Bjerg, P.L. In Situ Chemical Oxidation of Contaminated Soil and Groundwater Using Persulfate: A Review. *Crit. Rev. Environ. Sci. Tech.* **2010**, *40*, 55–91. [[CrossRef](#)]
16. Kitis, M. Disinfection of wastewater with peracetic acid: A review. *Environ. Int.* **2004**, *30*, 47–55. [[CrossRef](#)]
17. Chen, S.; Cai, M.Q.; Liu, Y.; Zhang, L.; Feng, L. Effects of water matrices on the degradation of naproxen by reactive radicals in the UV/peracetic acid process. *Water Res.* **2019**, *150*, 153–161. [[CrossRef](#)]
18. Zhang, C.; Brown, P.J.B.; Hu, Z. Thermodynamic properties of an emerging chemical disinfectant, peracetic acid. *Sci. Total. Environ.* **2018**, *621*, 948–959. [[CrossRef](#)]
19. Cai, M.; Sun, P.; Zhang, L.; Huang, C.H. UV/Peracetic Acid for Degradation of Pharmaceuticals and Reactive Species Evaluation. *Environ Sci Technol.* **2017**, *51*, 14217–14224. [[CrossRef](#)]
20. Lee, W.N.; Huang, C.H. Formation of disinfection byproducts in wash water and lettuce by washing with sodium hypochlorite and peracetic acid sanitizers. *Food Chem. X.* **2019**, *1*, 100003. [[CrossRef](#)]
21. Chhetri, R.K.; Baun, A.; Andersen, H.R. Acute toxicity and risk evaluation of the CSO disinfectants performic acid, peracetic acid, chlorine dioxide and their by-products hydrogen peroxide and chlorite. *Sci. Total. Environ.* **2019**, *677*, 1–8. [[CrossRef](#)]
22. Shah, A.D.; Liu, Z.Q.; Salhi, E.; Höfer, T.; Werschkun, B.; von Gunten, U. Formation of disinfection by-products during ballast water treatment with ozone, chlorine, and peracetic acid: Influence of water quality parameters. *Environ. Sci. Water Res. Tech.* **2015**, *1*, 465–480.
23. Zhao, X.; Zhang, T.; Zhou, Y.; Liu, D. Preparation of peracetic acid from hydrogen peroxide. *J. Mol. Catal. A Chem.* **2007**, *271*, 246–252. [[CrossRef](#)]
24. Sun, P.Z.; Zhang, T.; Mejia-Tickner, B.; Zhang, R.; Cai, M.; Huang, C.H. Rapid Disinfection by Peracetic Acid Combined with UV Irradiation. *Environ. Sci. Tech. Lett.* **2018**, *5*, 400–404. [[CrossRef](#)]
25. Du, P.; Liu, W.; Cao, H.; Zhao, H.; Huang, C.H. Oxidation of amino acids by peracetic acid: Reaction kinetics, pathways and theoretical calculations. *Water Res X.* **2018**, *1*, 100002. [[CrossRef](#)]
26. Zhang, K.; Zhou, X.; Du, P.; Zhang, T.; Cai, M.; Sun, P.; Huang, C.H. Oxidation of beta-lactam antibiotics by peracetic acid: Reaction kinetics, product and pathway evaluation. *Water Res.* **2017**, *123*, 153–161. [[CrossRef](#)]
27. Ina, E.V.R.; Makarova, K.; Golovina, E.A.; As, H.V.; Virkutyte, J. Free Radical Reaction Pathway, Thermochemistry of Peracetic Acid Homolysis, and Its Application for Phenol Degradation: Spectroscopic Study and Quantum Chemistry Calculations. *Environ. Sci. Tech.* **2010**, *44*, 6815–6821.
28. Rothbart, S.; Ember, E.E.; Van, E.R. Mechanistic studies on the oxidative degradation of Orange II by peracetic acid catalyzed by simple manganese(ii) salts. Tuning the lifetime of the catalyst. *New J. Chem.* **2012**, *36*, 732–748. [[CrossRef](#)]
29. Rokhina, E.V.; Makarova, K.; Lahtinen, M.; Golovina, E.A. Ultrasound-assisted MnO₂ catalyzed homolysis of peracetic acid for phenol degradation: The assessment of process chemistry and kinetics. *Chem. Eng. J.* **2013**, *221*, 476–486. [[CrossRef](#)]
30. Luukkonen, T.; Pehkonen, S.O. Peracids in water treatment: A critical review. *Crit. Rev. Environ. Sci. Tech.* **2016**, *47*, 1–39. [[CrossRef](#)]
31. Wang, Z.; Wang, J.; Xiong, B.; Bai, F.; Wang, S.; Wan, Y.; Zhang, L.; Xie, P.; Wiesner, M.R. Application of Cobalt/Peracetic Acid to Degrade Sulfamethoxazole at Neutral Condition: Efficiency and Mechanisms. *Environ. Sci. Tech.* **2020**, *54*, 464–475. [[CrossRef](#)] [[PubMed](#)]
32. Sharma, S.; Mukhopadhyay, M.; Murthy, Z.V.P. Degradation of 4-Chlorophenol in Wastewater by Organic Oxidants. *Ind.Eng.Chem.Res.* **2010**, *49*, 3094–3098. [[CrossRef](#)]
33. Zhou, F.; Lu, C.; Yao, Y.; Sun, L.; Gong, F.; Li, D.; Pei, K.; Lu, W.; Chen, W. Activated carbon fibers as an effective metal-free catalyst for peracetic acid activation: Implications for the removal of organic pollutants. *Chem. Eng. J.* **2015**, *281*, 953–960. [[CrossRef](#)]
34. Kim, J.; Zhang, T.; Liu, W.; Du, P.; Dobson, J.T.; Huang, C.H. Advanced Oxidation Process with Peracetic Acid and Fe(II) for Contaminant Degradation. *Environ. Sci. Technol.* **2019**, *53*, 13312–13322. [[CrossRef](#)]
35. Sun, H.Q.; Kwan, C.K.; Suvorova, A.; Ming, H.; Moses, A. Catalytic oxidation of organic pollutants on pristine and surface nitrogen-modified carbon nanotubes with sulfate radicals. *Appl. Catal. B Environ.* **2014**, *154–155*, 134–141. [[CrossRef](#)]
36. Guo, H.C.; Zhou, X.F.; Zhang, Y.L.; Yao, Q.F.; Qian, Y.J.; Chu, H.Q.; Chen, J.B. Carbamazepine degradation by heterogeneous activation of peroxymonosulfate with lanthanum cobaltite perovskite: Performance, mechanism and toxicity. *J. Environ. Sci.* **2020**, *91*, 10–21. [[CrossRef](#)] [[PubMed](#)]

37. Wang, Y.; Ren, J.; Wang, Y.; Zhang, F.; Liu, X.; Guo, Y.; Lu, G. Nanocasted Synthesis of Mesoporous LaCoO₃ Perovskite with Extremely High Surface Area and Excellent Activity in Methane Combustion. *J. Phys. Chem. C* **2008**, *112*, 15293–15298. [[CrossRef](#)]
38. Dacquin, J.P.; Dujardin, C.; Granger, P. Surface reconstruction of supported Pd on LaCoO₃: Consequences on the catalytic properties in the decomposition of N₂O. *J. Catal.* **2008**, *253*, 37–49. [[CrossRef](#)]
39. Pang, X.; Guo, Y.; Zhang, Y.; Xu, B.; Qi, F. LaCoO₃ perovskite oxide activation of peroxymonosulfate for aqueous 2-phenyl-5-sulfobenzimidazole degradation: Effect of synthetic method and the reaction mechanism. *Chem. Eng. J.* **2016**, *304*, 897–907. [[CrossRef](#)]
40. Taran, O.P.; Ayusheev, A.B.; Ogorodnikova, O.L.; Prosvirin, I.P.; Isupova, L.A.; Parmon, V.N. Perovskite-like catalysts LaBO₃ (B = Cu, Fe, Mn, Co, Ni) for wet peroxide oxidation of phenol. *Appl. Catal. B Environ.* **2016**, *180*, 86–93. [[CrossRef](#)]
41. Li, C.X.; Wu, J.E.; Peng, W.; Fang, Z.F.; Liu, J. Peroxymonosulfate activation for efficient sulfamethoxazole degradation by Fe₃O₄/β-FeOOH nanocomposites: Coexistence of radical and non-radical reactions. *Chem. Eng. J.* **2019**, *365*, 904–914. [[CrossRef](#)]
42. Wang, S.Z.; Xu, L.J.; Wang, J.L. Nitrogen-doped graphene as peroxymonosulfate activator and electron transfer mediator for the enhanced degradation of sulfamethoxazole. *Chem. Eng. J.* **2019**, *375*, 122041. [[CrossRef](#)]
43. Gkika, C.; Petala, A.; Frontistis, Z. Heterogeneous activation of persulfate by lanthanum strontium cobaltite for sulfamethoxazole degradation. *Catal. Today*. **2020**. [[CrossRef](#)]
44. Oh, W.D.; Chang, V.W.C.; Lim, T.T. A comprehensive performance evaluation of heterogeneous bi2fe4o9/p peroxymonosulfate system for sulfamethoxazole degradation. *Environ. Sci. Pollut. Res.* **2017**, *26*, 1026–1035. [[CrossRef](#)] [[PubMed](#)]
45. Lalas, K.; Petala, A.; Frontistis, Z. Sulfamethoxazole degradation by the CuOx/persulfate system. *Catal. Today*. **2020**. [[CrossRef](#)]
46. Yan, J.F.; Li, J.; Peng, J.L. Efficient degradation of sulfamethoxazole by the CuO@Al₂O₃ (EPC) coupled PMS system: Optimization, degradation pathways and toxicity evaluation. *Chem. Eng. J.* **2019**, *359*, 1097–1110. [[CrossRef](#)]
47. Hammouda, H.; Kalliola, S.; Sillanpaa, S.; Safaei, M.; Zhao, Z. Degradation and mineralization of phenol in aqueous medium by heterogeneous monopersulfate activation on nanostructured cobalt based-perovskite catalysts ACoO(3) (A = La, Ba, Sr and Ce): Characterization, kinetics and mechanism study. *Appl. Catal. B Environ.* **2017**, *215*, 60–73. [[CrossRef](#)]
48. Duan, X.G.; Su, C.; Miao, J.; Zhong, Y.; Shao, Z.; Wang, S.; Sun, H. Insights into perovskite-catalyzed peroxymonosulfate activation: Maneuverable cobalt sites for promoted evolution of sulfate radicals. *Appl. Catal. B Environ.* **2018**, *220*, 626–634. [[CrossRef](#)]
49. Hill, R.T. Decomposition of peracetic acid catalyzed by cobalt(II) and vanadium(V). *Can. J. Chem.* **1998**, *76*, 1064–1069.
50. Kim, J.; Du, P.; Liu, W.; Luo, C.; Zhao, H.; Huang, C.H. Cobalt/Peracetic Acid: Advanced Oxidation of Aromatic Organic Compounds by Acetylperoxyl Radicals. *Environ. Sci. Technol.* **2020**, *54*, 5268–5278. [[CrossRef](#)]
51. Zhang, Y.; Liu, J.; Moores, A.; Ghoshal, S. Transformation of Fluorotelomer Sulfonate by Cobalt(II)-Activated Peroxymonosulfate. *Environ. Sci. Technol.* **2020**, *54*, 4631–4640. [[CrossRef](#)] [[PubMed](#)]

Sample Availability: Samples of the lanthanum cobaltite perovskite are available from the authors.



© 2020 by the authors. Licensee MDPI, Basel, Switzerland. This article is an open access article distributed under the terms and conditions of the Creative Commons Attribution (CC BY) license (<http://creativecommons.org/licenses/by/4.0/>).